Building a 3D gravity-based model of the North Chilean subduction zone constrained by recent seismic results

INSTITUTE OF GEOPHYSICS OF THE CZECH ACADEMY OF SCIENCES

Dominika Godová[1], Christian Sippl[1] and Andrés Tassara[2]

[1]Institute of Geophysics of the Czech Academy of Sciences, Prague, Czechia (dgodova@ig.cas.cz)
[2]Universidad de Concepción, Departamento Ciencias de la Tierra, Concepción, Chile

Departamento de Ciencias de la Tierra, Universidad de Concepción

IPOC (Integrated Plate boundary Observatory Chile) network has enabled a range of studies that provided constraints on the geometry of the subduction zone in Northern Chile. To summarize these diverse constraints, we compiled a 3D integrated geophysical model of the region using IGMAS+, based on gravity data from the global gravitational model EIGEN-6C4 [1] (Fig. 1). Since the model covers both onshore and offshore areas, topography and bathymetry data from ETOPO2022 [2] were used during the process. The geometry and structure of the model stem from previous studies [3,4], where the main constraints were obtained by seismic data. We updated the model to fit the most up-to-date results from seismic, joint inversion, isostatic, and magnetotelluric studies wherever possible.

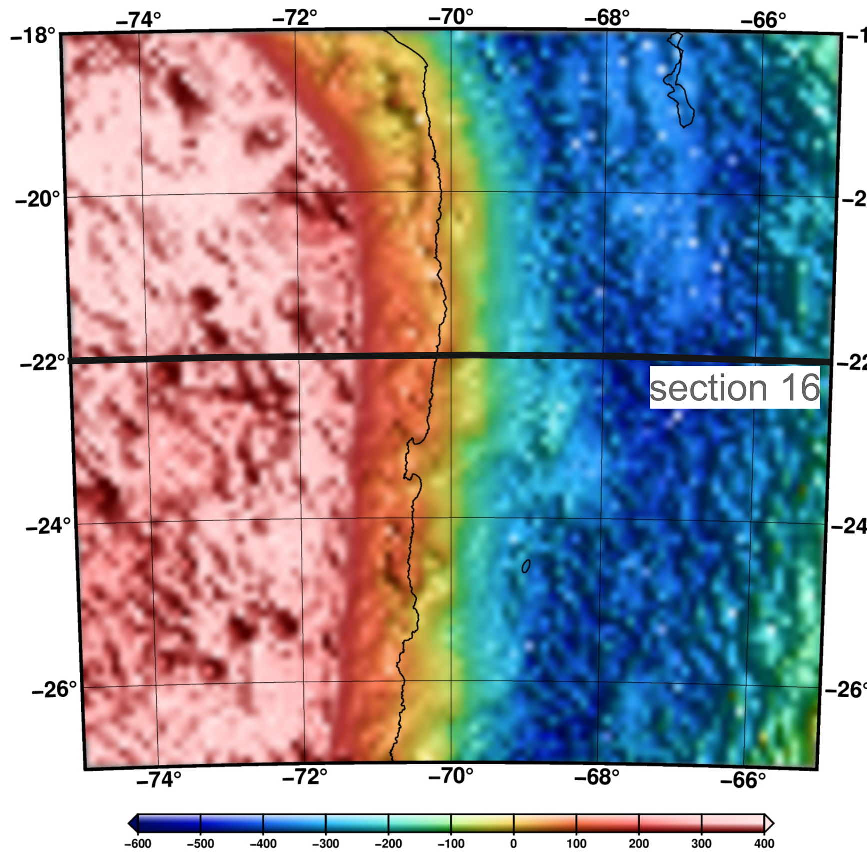

Fig. 1: Complete Bouguer Anomaly within the modelled area computed with 0.1° grid step by Calculation Service of the International Centre for Global Earth Models (ICGEM) from EIGEN-6C4 Global Gravity Field Model. Above, the model's position is shown within the geographical map of South America. The thick line shows section 16, which was selected to describe our model.

Fig. 2: A 3D view of our model from SE. Section 16 (at 22°S), on which the detailed structure is shown, is marked to show its position within the model.

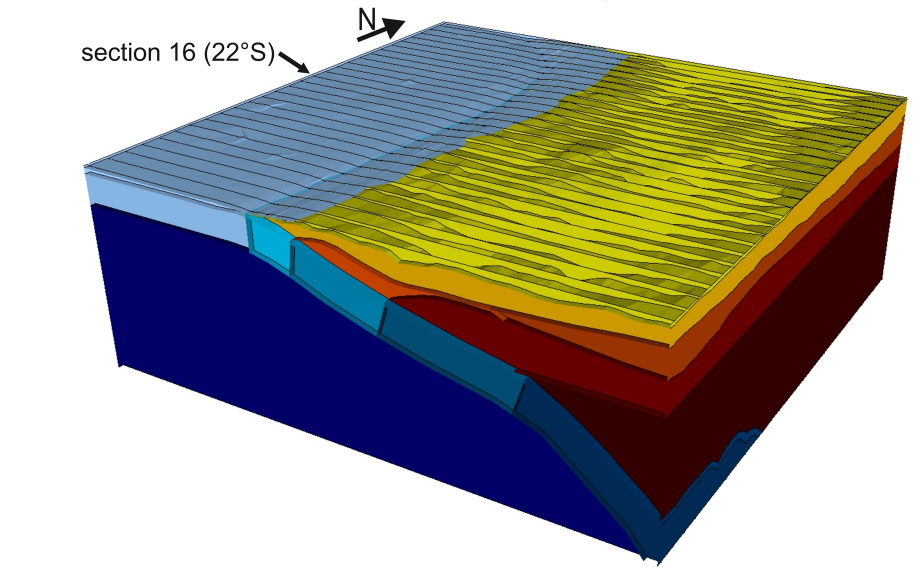

Fig. 3: a) An example of a 2D section of the model up to ~300 km depth, specifically section 16 located at 22°S. Numbers in brackets represent the densities of specific bodies in g·cm^{-3}. The density used for a reference body is 2.67 g·cm^{-3}. The continental upper mantle is split into two separate bodies representing two different domains of the deep crustal structure, where the cold mantle below the Andean foreland and shield regions (eastern part) has higher densities compared to the hot volcanic arc underneath the forearc region (western part). The slab consists of four separate parts (a-d) representing the probable changes of density values with depth. ICD (intracrustal density discontinuity), cM (continental Moho), and cLAB (continental lithosphere-asthenosphere boundary) together with respective lines highlight the main continental discontinuities. Slab divided into segments a-d is shown with densities for different parts (eg. a-OC - part a, oceanic crust; b-OM - part b, oceanic mantle). OC - oceanic crust, OM - oceanic mantle, WUM - western part of the continental upper mantle, EUM - eastern part of the continental upper mantle. Below, the same section is shown with: b) - seismic events (green dots) of the IPOC catalog [5] in the vicinity of the section (+/- 50 km around the section), and c) - original interface geometries [3,4] for oceanic Moho (red), oceanic LAB (yellow), slab (magenta), continental Moho (green), and ICD (blue).

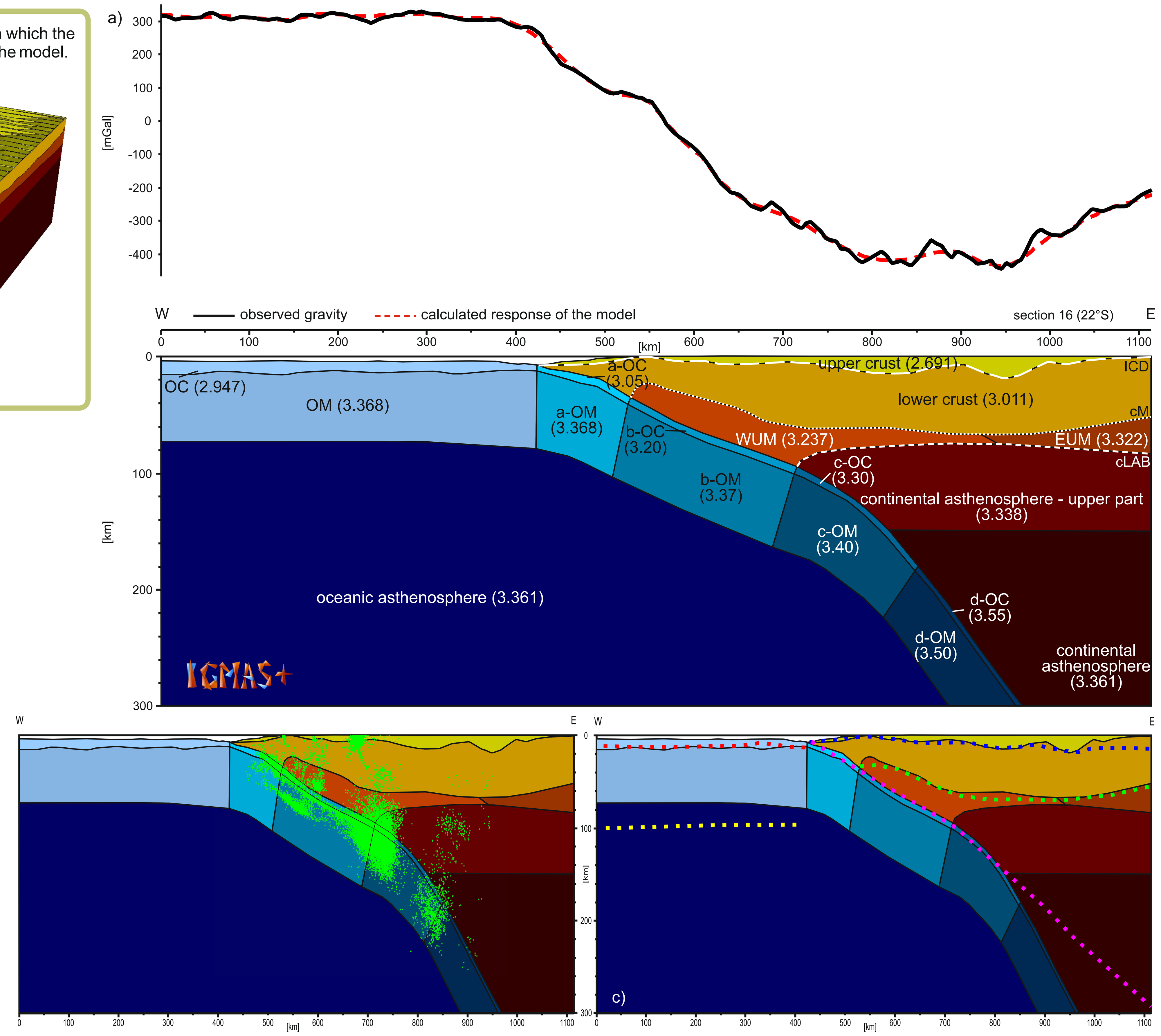

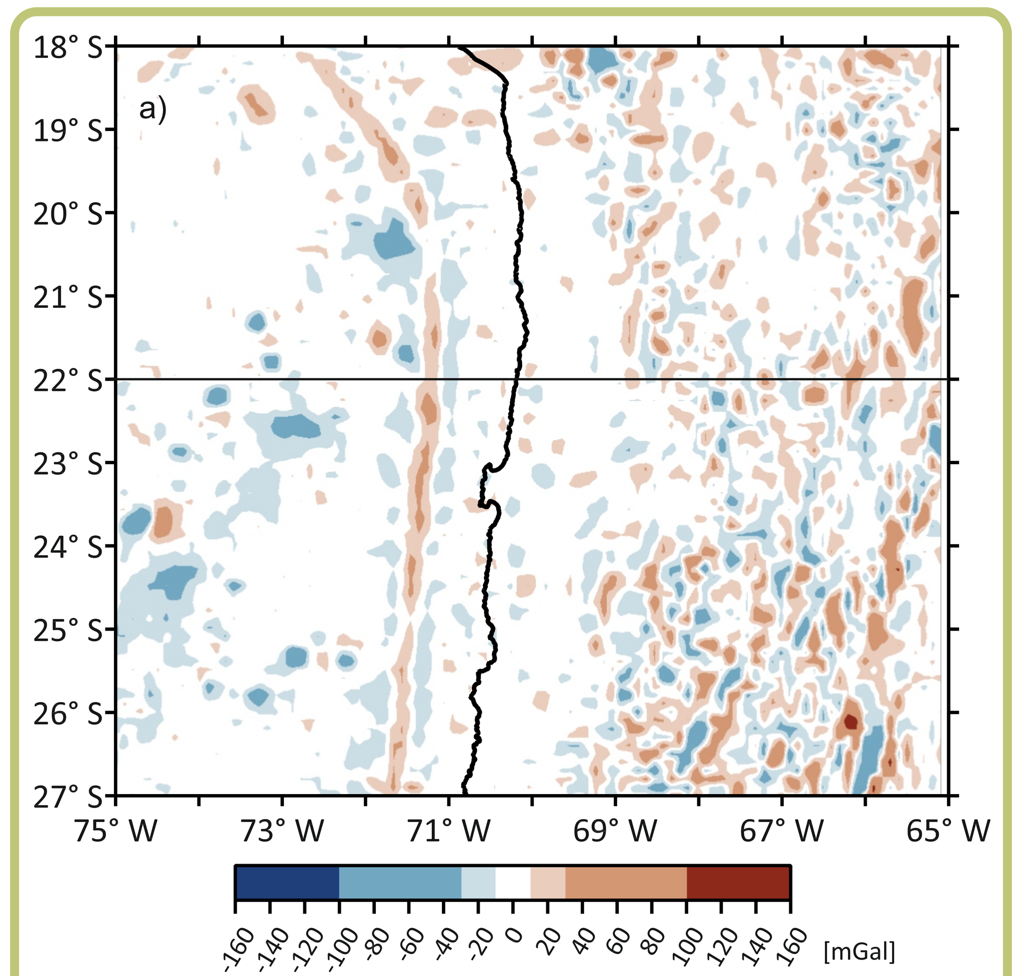

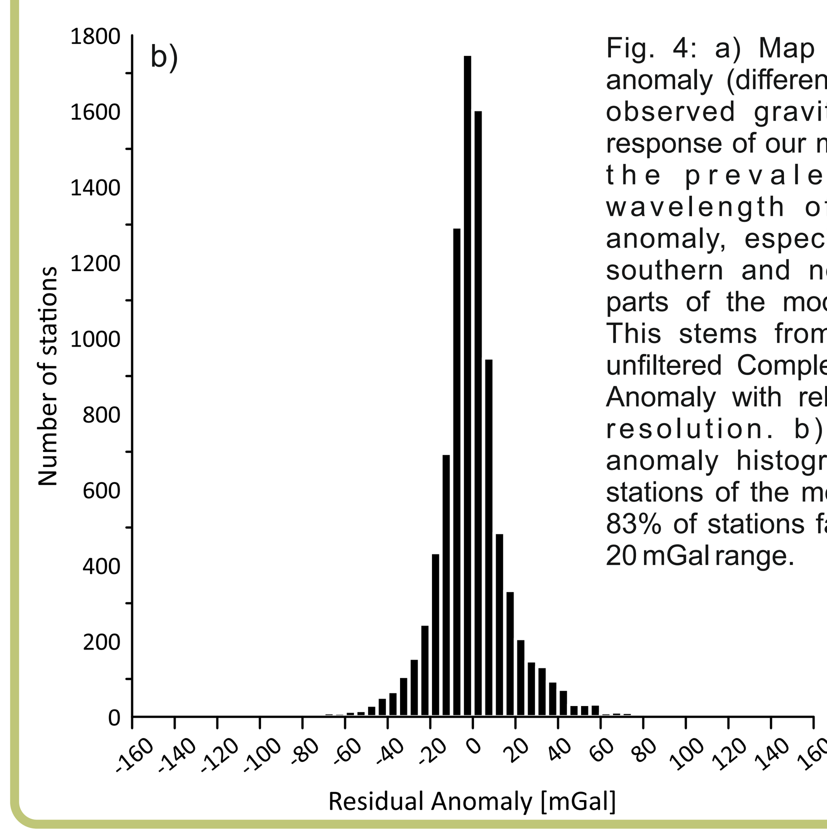

Fig. 4: a) Map of residual anomaly (difference between observed gravity and the response of our model). Note the prevalent short wavelength of residual anomaly, especially in the southern and northeastern parts of the modelled area. This stems from using the unfiltered Complete Bouguer Anomaly with relatively high resolution. b) Residual anomaly histogram for the stations of the model. Nearly 83% of stations fall within +/- 20 mGal range.

General model description

Our 3D model (Fig. 2) extends from 75°W to 65°W and from 17°S to 27°S (Fig. 1). It consists of 28 evenly distributed (with a step of ~0.33°) W-E oriented parallel 2D sections with a depth of 410 km. Each section includes six continental bodies, three oceanic realm bodies, and eight bodies of the slab (Fig. 3). The residual anomaly is shown in Fig. 4.

Modifications to the initial model

The geometry and density of an initial model were based on previous studies [3,4]. Our aim was to update these to fit the recent datasets for specific interfaces - especially the slab, the Moho, and the lithosphere-asthenosphere boundary (LAB) for both oceanic and continental plates. We modified these interfaces based on selected datasets with the most complete, relevant, and up-to-date information available.

Geometry

Recent data from the IPOC (Integrated Plate Boundary Observatory Chile) seismicity catalog [5] enabled us to refine the top of the slab together with a recent dataset [6] that improves the geometry in the shallow part of the slab. The oceanic Moho was adjusted to obtain a better fit to the observed gravity to a reasonable level to be consistent with recent studies [7]. As for the oceanic LAB, we decided to keep it more consistent with the results of multiple studies [8] and to keep the lithospheric thickness constant throughout its whole extent. Continental Moho in our model was modified to fit the compilation dataset of crustal thickness studies within South America [9]. ICD was adjusted to improve the fit between the observed gravity anomaly and the calculated response of our model. We decided to keep the geometry of the continental LAB the same as in a previous model [4].

Densities

Note that our densities differ from the original ones [3,4]. We used a single reference body with a density of 2.67 g·cm^{-3}, while in the original studies [3,4] a layered background reference model was used. The main differences are in the asthenospheric bodies, the oceanic crust, and the lower crust of the continental plate. These modifications were done to improve a fit of the model's response to the observed gravity and were fine-tuned by the results of the inversion tool feature in IGMAS+.

Fig. 5: The bathymetry of the modelled area extracted from the ETOPO2022 dataset [2] overlayed by contours of the thickness of the oceanic crust of our model. Note a good correlation of higher bathymetry represented by Iquique ridge and surrounding seamounts with increased thickness of the modelled oceanic crust.

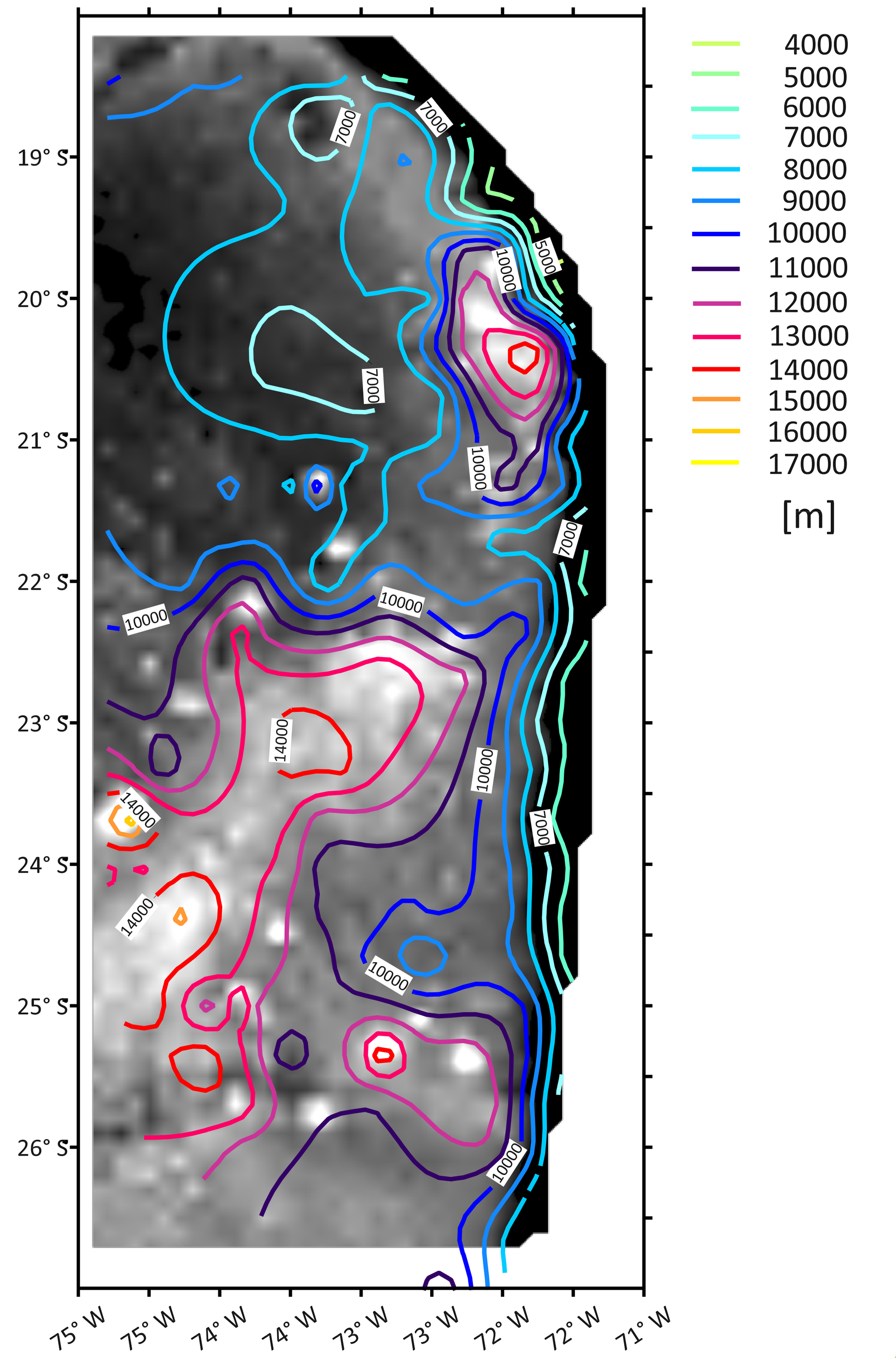

Comparing the thickness of the oceanic crust to bathymetry

The oceanic Moho in our model goes up to a depth of 19,5 km (below the surface of the model). We decided to translate this to a crustal thickness, which can be increased in the areas of high bathymetry (the Iquique ridge, seamounts) up to about twice the average thickness of the oceanic crust [8]. We compared our oceanic crustal thickness with bathymetry in Fig. 5. Note the good correlation between increased thickness and the occurrence of higher bathymetry.

Mantle wedge - is it really there?

We compared multiple seismic constraints for continental Moho and found a great variance in its geometry, especially in the area of mantle wedge occurrence in previous models [3,4]. To test the need for its presence, we calculated the response of our continental Moho geometry with a mantle wedge, and a "flat" continental Moho (Fig. 6). The misfit between these two scenarios is about 200 mGal. Improvng the misfit in our model would require either increasing the density, which would translate to a misfit in the rest of the model, or adjusting the ICD, which is already very shallow. Therefore, our results suggest the presence of the mantle wedge near the plate interface.

Fig. 6: a) A comparison of a response of the continental Moho geometry as modelled in our work (pink) to a scenario of a "flat" continental Moho without a mantle wedge in section 16. Two possible options for fitting the ~200 mGal misfit between the "mantle wedge" and the "flat" Moho scenarios are shown in b) and c). In b) we tried to improve the misfit by increasing the density of the lower crust from 3.011 g·cm^{-3} to 3.15 g·cm^{-3} to show that it would be impossible to improve the fit only by modifying the density of the nearest body above the interface (continental Moho). In c) we tried to fit the difference by adjusting the ICD geometry. Note that a good fit could not be obtained due to already shallow ICD geometry prior to this modification.

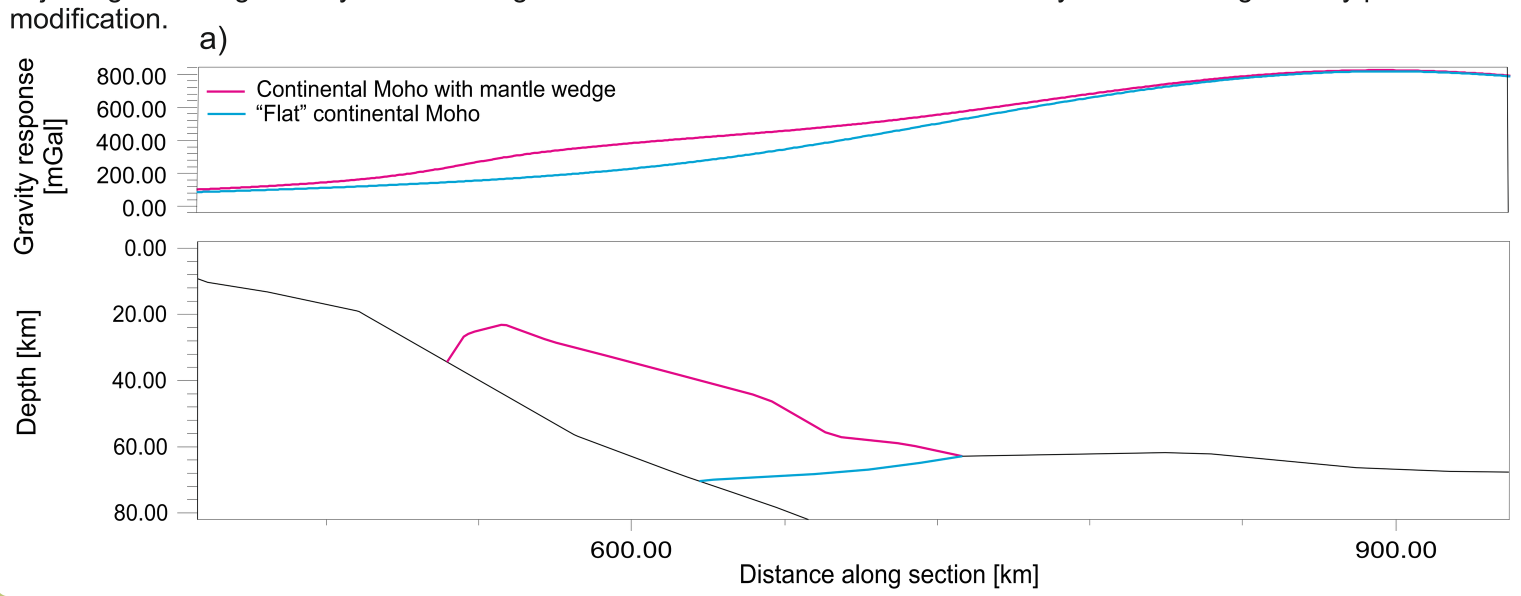

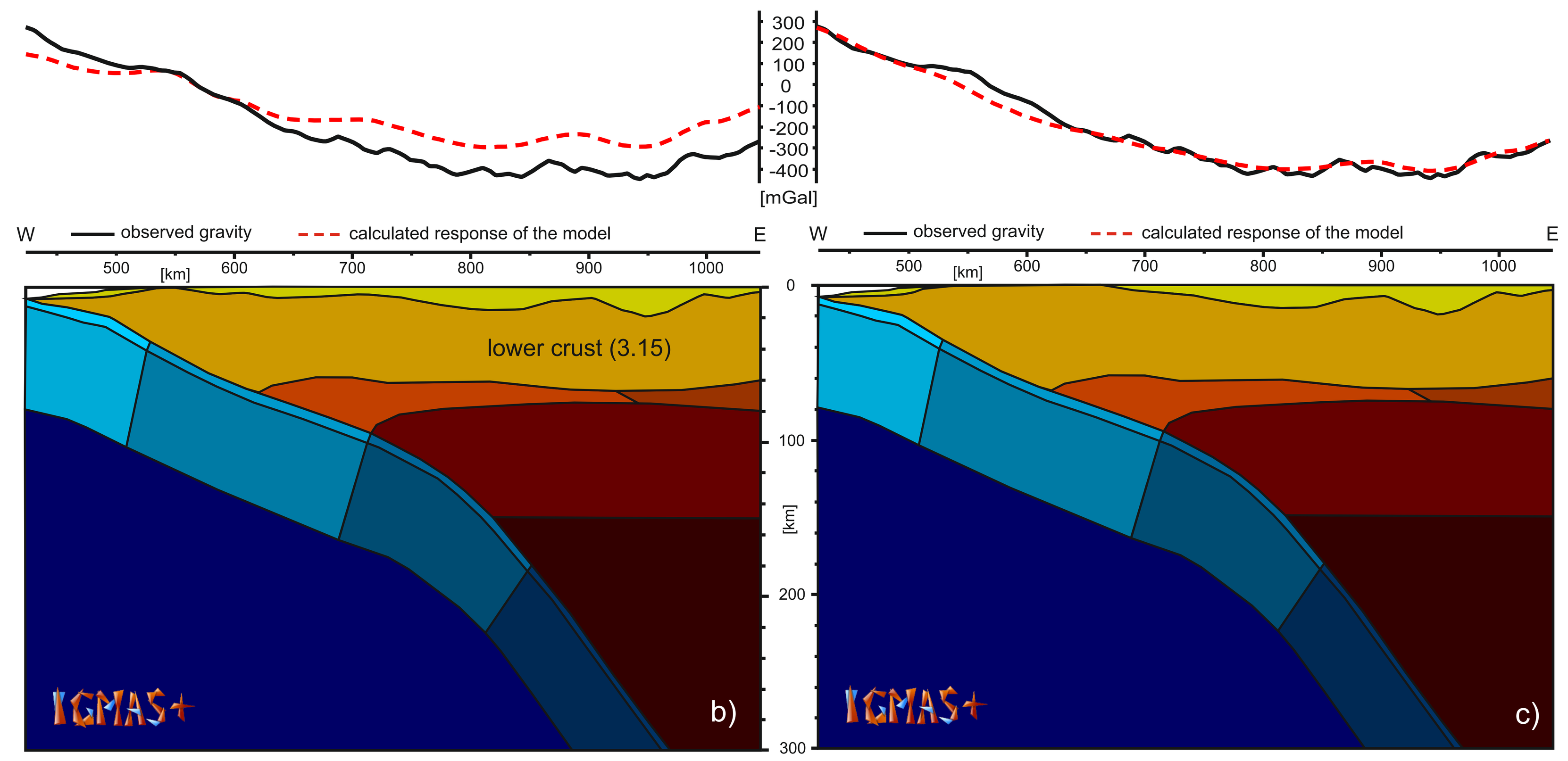

Acknowledgement: C. Sippl has received funding from the European Research Council (ERC) under the European Union's Horizon 2020 research and innovation programme (ERC Starting Grant MILESTONE; StG2020-947856). The research was also supported by Fondecyt 1240862 Crustal Rheology, Deformation and Seismicity of the Andean Margin.

References: [1] Foerste, Ch., et al. (2014): EIGEN-6C4 The latest combined global gravity field model including GOCE data up to degree and order 2190 of GFZ Potsdam and GRGS Toulouse, GFZ Data Services; [2] NOAA National Centers for Environmental Information (2022): ETOPO 2022 15 Arc-Second Global Relief Model [accessed 2024-01-11]; [3] Tassara, A, et al. (2006): Three-dimensional density model of the Nazca plate and the Andean continental margin. J. Geophys. Res., 111, B09404; [4] Tassara and Echaurren (2012): Anatomy of the Andean subduction zone: three-dimensional density model upgraded and compared against global-scale models. Geophys. J. Int., 189, p. 161-168; [5] Sippl, Ch., et al. (2018): Seismicity Structure of the Northern Chile Forearc From >100,000 Double-Difference Relocated Hypocenters. J. Geophys. Res. Solid Earth, 123, p. 4063-2087; [6] Contreras-Reyes, E., et al. (2025): Offshore geometry of the South America subduction zone plate boundary. Earth Planet. Sci., 651, 119175; [7] Contreras-Reyes, E., et al. (2021): Density structure, flexure, and tectonics of the Iquique Ridge, northern Chile. J. South Am. Earth Sci., 111, 103423; [8] Steinberger, B. & Becker, T. W. (2018): A comparison of lithospheric thickness models. Tectonophysics, 746, p. 325-338; [9] Rivadeneyra-Vera, C., et al. (2019): An Updated Crustal Thickness Map of Central South America Based on Reciever Function Measurements in the Region of the Chaco, Pantanal, and Paraná Basins, Southwestern Brasil. J. Geophys. Res.: Solid Earth, 124, p. 8491-8505.